

Elastic Deformation Analysis of the Blade Workpiece in the Milling Process with a Disk-Shaped Cutter

Xinfeng LIU^a, Riliang LIU^{a,1} and Jiaming FENG^a

^a *School of Mechanical Engineering, Shandong University, Jinan, 17923 Jingshi Road, Shandong, China*

Abstract. Turbine blades play a decisive role in the performance of turbomachinery. The whirling milling process may provide a cost-effective way to produce blade surfaces. However, due to the low stiffness of blades, elastic deformation of the workpiece is often induced by the cutting force during the blade whirling process. In this paper, the elastic deformation in finish machining blades using a disk-shaped milling cutter on a 3-axis (C/Z/X) CNC machine is investigated. First, the process of the blade-whirling is briefly introduced. Then, the simulation model is established for analysis of the elastic deformation of the workpiece. Seven sections are made along the blade and twenty reference points are set in each section. By applying forces to these points, the deformations at the different location of the blade surface are analysed by means of simulation using the ABAQUS software. The deformation trend and the maximum displacements of the workpiece are identified, which is of great significance for improving the manufacturing quality and efficiency.

Keywords: Cutting deformation, turbine blades, whirling process, disc-shaped milling cutter, finite element simulation.

1. Introduction

Blades are essential components for turbomachines to transfer or convert energy and play a decisive role in their performance [1]. In modern industry, these blades are often designed with freeform surfaces featuring large torsion angle, thin wall structure and tight tolerance, to maximize the working efficiency of the machine [2,3]. The manufacture of the blade surfaces is usually produced by five-axis computerized numerically controlled (CNC) milling and polishing.

Although five-axis machining is a developed technology, its high cost in terms of machine tools and manpower impairs its application in small and medium-sized enterprises. Consequently, a number of alternative approaches have been proposed in order to get the blades machined on three-or four-axis machines, including the spiral milling on a regular three-axis CNC machine combined with an automatic indexing rotary table [4], the turn-milling on a four-axis machine [5], and the whirling milling process with a disc-mill cutter on a thread-whirling machine [6].

Due to the large rotary diameter of the cutting tool, the whirling process features higher cutting speed and thus less machining time than ordinary milling [6]. However,

¹Corresponding author: Riliang Liu, E-mail: liuriliang@sdu.edu.cn

the blade whirling process is also prone to workpiece deformation by the cutting force, cutting heat, residual stress, clamping positioning, clamping force, tool tip wear, machining vibration and other factors in this process [7,8]. Although quite a number of papers have covered the deformation of blade, most of them focused on the five-axis milling with an end mill or flank mill. They mainly focused on deformation prediction and compensation of the deflection errors [9]. Generally, the cutting force model is firstly established according to the cutter workpiece engagement analysis [10], followed by the computation of workpiece deformation and cutter deformation, which are combined to obtain the total deformation error [11] and then the compensation value. Due to the complex surface of the thin-walled parts, the finite element method is usually used to compute the deformation [12,13]. This paper will focus on the whirling milling process with a disk-shaped cutting tool employed to produce the blade surfaces on a three-axis (C/Z/X) CNC machine.

2. The Blade Whirling Process

The blade whirling operation can be understood as the machining process in which the blade surface is cut from a rectangular blank point by point on a three-axis CNC machine through appropriate selection of cutting-edge geometry and tool path for the disc-shaped milling cutter, as shown in Figure 1. In order to produce the complicated blade surface, the whirling unit of the machine is equipped with a disc-shaped milling cutter with a number of appropriate cutting-edges, which is powered by a separate motor rotating at high speed to remove excess material from the blank. The machine tool contains two linear axes Z and X for cutter's feed motion. During the whirling operation, the workpiece rotates with the machine spindle at low speed, in the same time, the disc cutter, while spinning at high speed, moves simultaneously along both Z and X axes following the NC program.

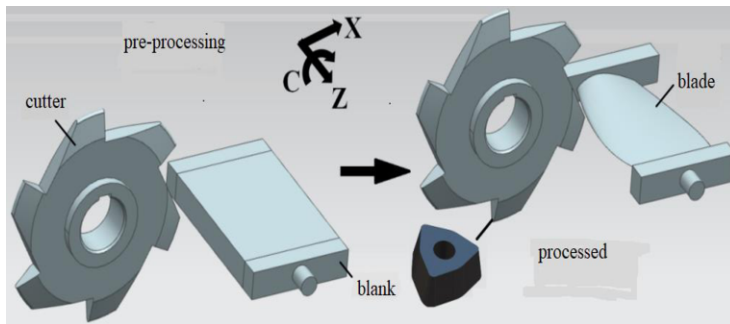


Figure 1. The blade whirling process.

It is worth mentioning that, from the rectangular blank to the final blade surface, three processes at least are needed, i.e. rough, semi-finish and finish machining. In the roughing stage, large material will be cut from the rectangular blank. In the final stage, only a small allowance is to be removed for the quality machining.

Figure 2 illustrates the whirling milling process (viewed in the Z direction), by showing the changing position and orientation of the workpiece in relation to the disk-shaped cutter at a few points. Throughout the operation both the workpiece and the cutting tool keep their centers' position unchanged in the Y- direction. It is via the

rotation of the workpiece in coordination with the cutting tool that enables cutting of the workpiece for different points in the Y-direction. In order for continuous cutting of the blade surface around its axis, spiral toolpath is adopted for the whole process. This makes the cutter continuously remove material along the same direction of the blade cross-section and ensures the consistency of the cutting process.

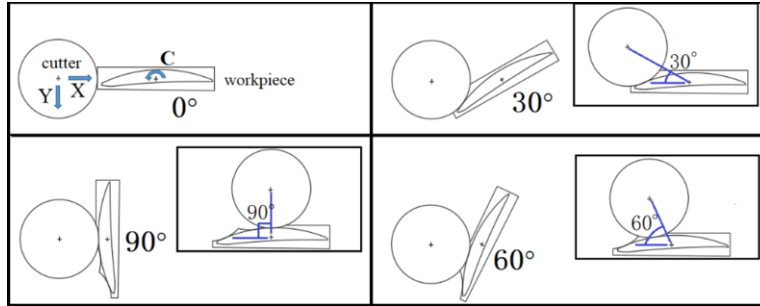


Figure 2. Relative position of workpiece and cutter during whirling process.

3. Simulation Model of Elastic Deformation in the Blade Whirling Process

3.1. Hypothesis for Finite Element Simulation

For simplicity, the following assumptions are made in the finite element analysis of the elastic deformation of the workpiece in the blade whirling process.

- The simulation is only for the finish machining process with small radial cutting depth. The simultaneous change in stiffness of the workpiece during material removal can be ignored.
- The process of cutting a workpiece at a CC point to form a single chip can be simplified to the process of applying an instantaneous concentrated force directly to the CC point (reference point) in order to simulate the elastic deformation of the blade in different area caused by the milling force applied by disc milling cutter.
- The influence of the initial residual stress of the material, the cutting heat and vibration generated in the machining process and the residual stress after cutting on the plastic deformation of the workpiece can be ignored.

3.2. Finite Element Modeling for Elastic Deformation Analysis

The Standard module of the ABAQUS 6.14 software is used to simulate the application of milling force in actual machining. Specific steps are as follows:

- Use CAD software for three-dimensional modeling of the blade, then save the model as .IGES file and import it into the ABAQUS software. After that assign parameters to the workpiece material H59 and the cutter carbide respectively.
- Define continuous static general analysis steps with the same number of reference points in a cross section. In the output of historical variables, establish the output of historical variables for all reference points on the same section. Check U under the column of displacement/velocity/acceleration column,

which will be expression of displacement generated by cutting force in the x, y and z directions in visualization module in the future.

- Define boundary constraints. In the simulation of the whirling processing, the workpiece is fixed by clamping device composed of three-jaw chuck and thimble, which limits except rotation around the spindle of the five degrees of freedom, meanwhile implements boundary constraints on the blade.
- Define load. Assuming that the cutting force in the machining process is a concentrated force, the concentrated force is applied on the reference points with corresponding numbers in each separate analysis step successively, meanwhile unload the applied force on the other reference points, so as to achieve the simulation effect. After that observe the displacement of the reference points for different location caused by the applied force, which is set according to the milling force measured by experiment.
- Mesh generation. In this paper, the Tet grid was used to divide the blade surface into C3D10 tetrahedral mesh cells, after grid division, the nodes are 7856 and the cells are 3227, as shown in Figure 3. To ensure the calculation accuracy and efficiency of the simulation results, mesh refinement was carried out in force application area of the workpiece. After submitting the task, the elastic deformation is obtained by applying the concentrated force to the reference point in the post-processing visualization module.

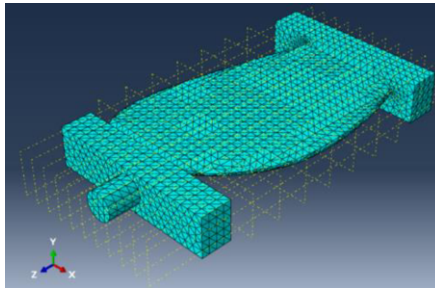


Figure 3. meshing of the blade.

3.3. Reference Point Setting

For analysis of the elastic deformation of the whole blade, the blade surface was divided into 7 reference planes by the interval $z=20\text{mm}$ along the z direction, the value is 60, 80, 100, 120, 140, 160 and 180mm respectively, as shown in Figure 4. Considering the feature that thin-wall curvature changes greatly at the leaf edge, sparse and unequal reference points were set on each section according to the length and curvature of the contour line, in this order, the same number of 20 reference points were set on each section. Figure 5 shows the distribution of reference points on the cross section $z=60\text{mm}$, in which the reference points are numbered in a counterclockwise order along the +z axis, so as the other reference planes.

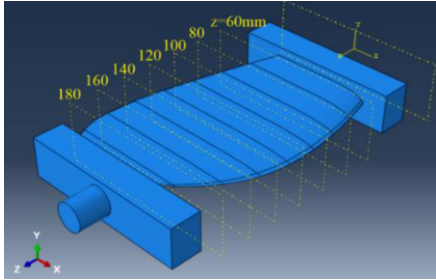


Figure 4. Reference plane setting on the blade surface.

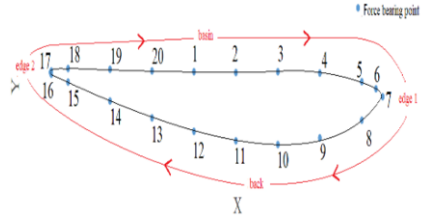


Figure 5. Distribution of the reference points on blade surface.

4. Elastic Deformation Analysis of the Blade in Whirling Process

Taking the twenty reference points in the reference plane $z=60\text{mm}$ and applying force to them respectively, the stress and deformation distribution of the blade surface can be simulated when the disc milling cutter cuts a circle around the workpiece in the reference plane, as shown in Figure 6.

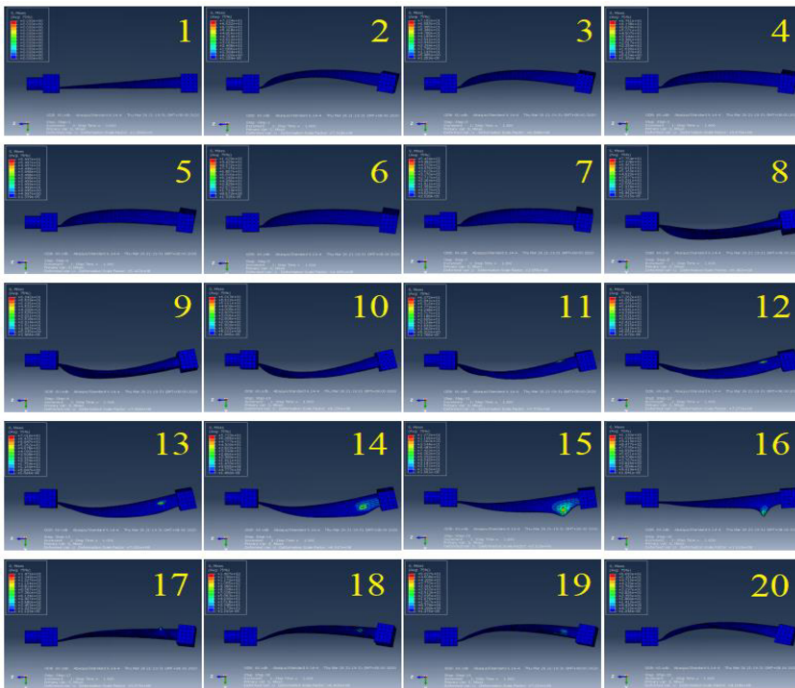


Figure 6. Schematic diagram of blade deformation at the twenty reference points.

4.1. The Chart of Deformation Trend and Maximum Displacement

The deformation of each reference point in the corresponding analysis step can be simply observed from the figure above. In order to more intuitively analyze the deformation rule, the displacement change of 20 reference points will be drawn in the visual module, which

is referred to as the deformation trend chart of the reference point. Since the elastic deformation is not obvious in the other two directions for the special structure of the blade, this paper only focuses on the elastic deformation in the y direction. Figure 7 shows the displacement and deformation trends of 20 reference points in the y-direction on the z=60mm plane, whose abscissa represents time, namely analysis steps 1 to 20, while the ordinate of which is the trend of the displacement of the reference. Each color represents a reference point, and positive or negative displacement represents the direction.

It can be observed from the deformation trend diagram that when a force is applied to the blade, all reference points have displacement changes, while the reference point in the same position will have different displacements corresponding to the force applied from different position. When the force is applied to the reference point 7 and 16 of the thin-walled blade edge, the maximum displacement peak appears, especially. Meanwhile, when the force is applied to point 7, whose nearby reference points, including point 5, 6, 7 and 8, will have a large displacement. Similarly, when the force is applied to pint 16, the reference point near 16 generates a large displacement. However, it is worth noting that when the force is applied to point 7, point 16 at the other edge of the blade body only generates a small displacement due to its distance, and vice versa. When the force is applied to the back of the blade or the basin, the displacement at all points is much smaller than applied at the edge, even at the applied position.

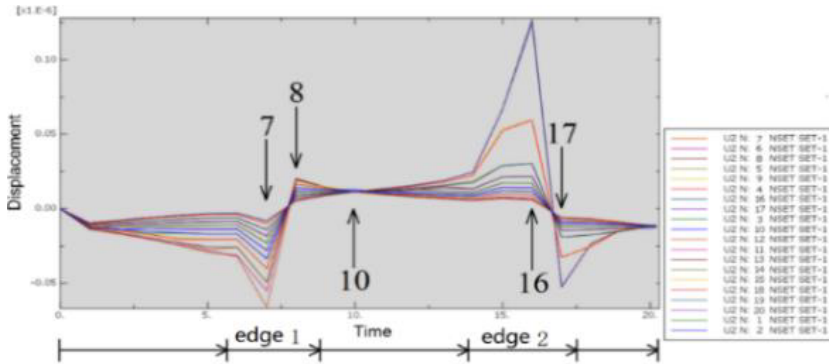


Figure 7. Deformation trend on the z=60mm plane.

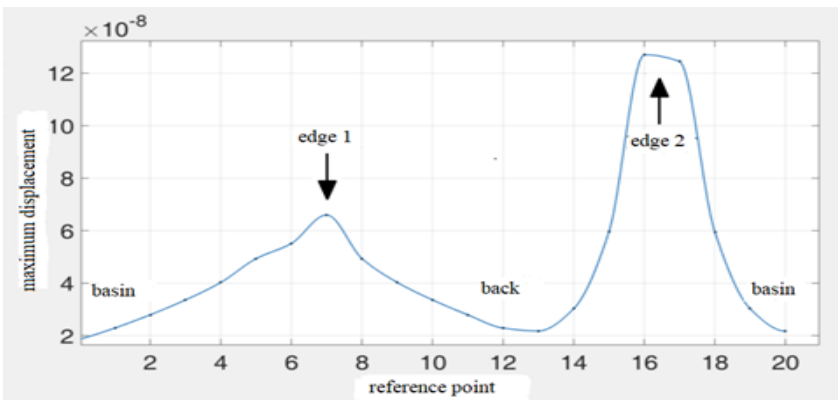


Figure 8. Schematic diagram of maximum displacement in the plane z=60mm

The deformation trend chart shows the deformation of all reference points at all analysis steps, where the maximum displacement value of each reference point in all analysis steps can be obtained. Fit these maximum values into a curve using MATLAB, which is called the maximum displacement curve of reference point, representing the maximum deformation at each reference point on a section, meanwhile, reflecting the influence of geometric shape on deformation. The maximum displacement curves of the twenty reference points on the cross section $z=60\text{mm}$ are shown in Figure 8.

It can be seen more intuitively from the diagram of the maximum displacement curve that the corresponding maximum deformation displacement value increases gradually when the position applied with force changes from the reference point 1 on the blade basin 1 to the reference point 7 at the thin wall of the blade edge, while reaches the maximum value at point 7. When the position applied with force changes from point 7 to the back of the blade, the corresponding maximum displacement value decreases, in addition, the decreasing rate is basically the same as the rising rate of process that the point applied with force move to point 7, while the minimum value occurs at the reference point 13. From reference point 14, the displacement increases rapidly, when near point 16 and point 17, the displacement reaches a maximum value, afterwards decreases rapidly to zero after passing this blade edge 2. To sum up, we can conclude that the displacement deformation at the blade basin and blade back is smaller than that at the blade edge, which is mainly caused by that the thin-wall curvature at the blade edge changes greatly, while the blade edge is farther away from the main axis than the blade back. According to the mechanics of materials, the bending deformation at the blade edge is larger, which accords with the mechanical deformation law, meanwhile the displacement at the corresponding reference points of the blade basin and blade back is basically equal in value. In addition, the maximum negative displacement deformation at step-7 is smaller than the maximum positive displacement deformation at step-16, on account of that the wall thickness of reference point 7 at blade edge 1 is larger than that of reference point 16 at blade edge 2.

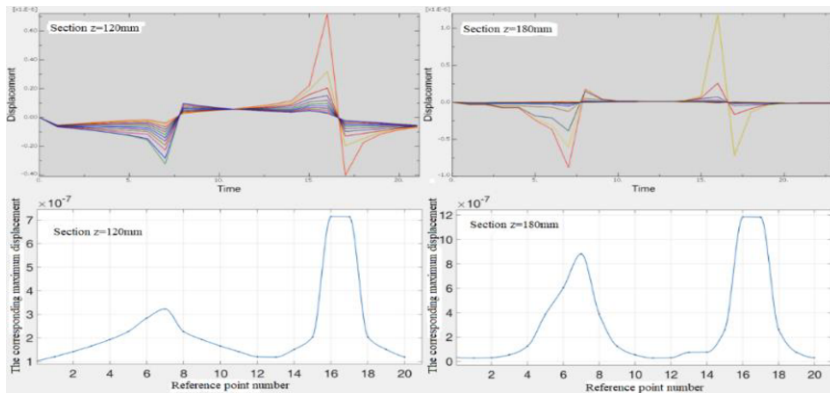


Figure 9. Deformation trend and maximum displacement on the planes $z=120\text{mm}$ and $z=180\text{mm}$.

In order to verify the accuracy of deformation law, the extra two simulations about the section $z=120\text{mm}$ and $z=180\text{mm}$ are carried out under the same conditions as preceding. Through the simulation results, the maximum displacement curves on these two sections are fitted, which indicates the consistency between the displacement variation trend and corresponding maximum displacement of reference points on the

cross-section of $z=120\text{mm}$ and $z=180\text{mm}$ and that of $z=60\text{mm}$. Whereas the value of the deformation exists difference, as shown in Figure 9.

4.2. Elastic Deformation Prediction Surface

In order to explore the deformation of the whole blade surface, the all 140 reference points on the 7 cross sections are selected for simulation, thus obtain the maximum displacement values of 140 reference points representing different positions, which were fitted with the Cubic method of MATLAB to obtain the prediction surface of three-dimensional blade force displacement and deformation, as shown in Figure 10. The maximum displacement of each reference point in all analysis steps is taken as the Z coordinate, the number of reference point is taken as the X coordinate, and the position of cross section is taken as the Y coordinate.

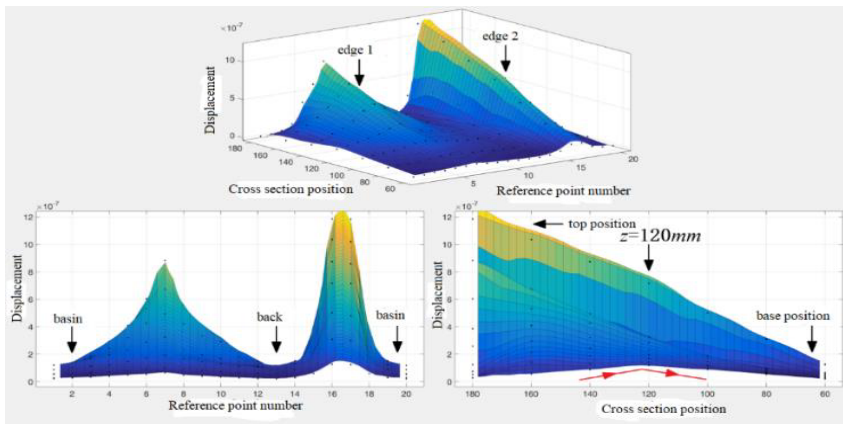


Figure 10. Blade surface deformation in three dimensions.

Due to the fact that the root of the blade ($z=60\text{mm}$) is fixed by the thimble, and the top of the blade ($z=180\text{mm}$) is fixed by the three-jaw chuck, the deformation of the two is supposed to be smaller than that of the middle of the blade ($z=120\text{mm}$), according to the mechanical principle. However, that does not match the results on Figure 10, which is caused by fact that the characteristics of the section and thickness of the tip of the blade are much smaller than other sections, while the deviation between the section center and the main shaft axis is larger. Therefore, the displacement and deformation shows an upward trend from the root to the tip of the blade. Due to the fixed clamping at both ends of the blade and the bending and twisting caused by the cutting force, the stress deformation of the blade is along the Y-axis. While the minimum displacement of the reference points on the seven sections presents an approximate inverted "V" shape distribution, that is, the minimum displacement of the reference points on the section at the middle of the blade ($z=120\text{mm}$) is the largest.

5. Conclusion

In this paper, blade whirling was investigated focusing on elastic deformation of the workpiece in the machining process. Based on the kinematics of the blade whirling process, the simulation model was made after necessary simplification for analysis of the

elastic deformation of workpiece. Then the deformation trend and maximum displacements were identified and analysed. The conclusion of the research work can be summarized into the following points.

- The proposed simulation model for the blade whirling process was capable of accurately predicting the elastic deformation of blade whirling.
- The elastic deformation in the whirling process was greatly affected by the blade shape. Identification of the rule of elastic deformation for a specific blade is of great significance to compensate the machining errors caused by elastic deformation.

The work in this paper enables quantitative simulation of the elastic deformation for blade whirling, which provides compensation for the error in the process. However, using the simplified model can only explain the validity of finite element model from the numerical relation. Future work will focus on other factors that induce elastic deformation and the methods of compensation.

Acknowledgments

This research was financially supported by the National Natural Science Foundation of China (NSFC, Grant NO. 52275494) and the Natural Science Foundation of Shandong Province, China (Grant No. ZR2021ME078).

References

- [1] Amini K and Heidari M Vibration Analysis of Steam Turbine Blade: A Finite Element Analysis. *Adv. Sci. Lett.* 2018; 24: 9026-30
- [2] Ye Z A systematic computational design system for turbine cascades, airfoil geometry, and blade-to-blade analysis. *J. Eng. Gas Turb. Power* 1984; 106: 598-605
- [3] Shen X, Chen J, Zhu X, Liu P and Du Z. Multi-objective optimization of wind turbine blades using lifting surface method. *Energy* 2015; 90: 1111-21
- [4] Shan C, Liu W, Lin X and Zhang D Three half-axis tool orientation optimization for spiral machining of blades *Int. J. Adv. Manuf. Technol.* 2013; 68: 2601-09
- [5] Ning J and Zhu L. Parametric design and surface topography analysis of turbine blade processing by turn-milling based on CAM. *Int. J. Adv. Manuf. Technol.* 2019; 104: 3977-90
- [6] Han L, Liu R, Liu X and Feng J. Theoretical modeling and chatter prediction for the whirling process of airfoil blades with consideration of asymmetric FRF and material removal. *Int. J. Adv. Manuf. Technol.* 2020; 106: 2613-28
- [7] Xiang J and Yi J. Deformation mechanism in wax supported milling of thin-walled structures based on milling forces stability. *CIRP-JMST* 2021; 32: 356-69
- [8] Li W, Wang L and Yu G. Force-induced deformation prediction and flexible error compensation strategy in flank milling of thin-walled parts. *J. Mater. Process Tech.* 2021; 297: 117258
- [9] Ge G, Xiao Y, Feng X and Du Z. An efficient prediction method for the dynamic deformation of thin-walled parts in flank milling. *Comput-Aided Des.* 2022; 152: 103401
- [10] Wang I and Si H. Machining deformation prediction of thin-walled workpieces in five-axis flank milling. *Int. J. Adv. Manuf. Technol.* 2018; 97: 4179-93
- [11] Altintas Y, Tuysuz O, Habibi M and Li Z. Virtual compensation of deflection errors in ball end milling of flexible blades. *CIRP Ann.* 2018; 67: 365-8
- [12] Huang N, Bi Q, Wang Y and Sun C. 5-axis adaptive flank milling of flexible thin-walled parts based on the on-machine measurement. *Int. J. Mach. Tools Manuf.* 2014; 84: 1-8
- [13] Wang J, Quan L and Tang K. A prediction method based on the voxel model and the finite cell method for cutting force-induced deformation in the five-axis milling process. *Comput. Methods Appl. Mech. Eng.* 2020; 367: 113110.